J Nanopart Res (2014) 16:2615
DOI 10.1007/s11051-014-2615-8

RESEARCH PAPER

Photocatalytic performance of melt-electrospun polypropylene fabric decorated with TiO_2 nanoparticles

Zeynep Karahaliloglu · Christoph Hacker · Murat Demirbilek · Gunnar Seide · Emir Baki Denkbas · Thomas Gries

Received: 3 May 2014 / Accepted: 19 August 2014 / Published online: 29 August 2014

Abstract Recently, nanomaterials, especially titanium-based nanomaterials, have a great potential for decolorization of textile dye effluents. In this article, the nanofibrillar filters functionalized with titanium nanoparticle (nTi) were designed to improve dyeing wastewater decolorization. Pristine polypropylene (PP) and nTi-PP nanocomposite nonwovens were produced as a photocatalyzer by melt-electrospinning process. The average diameter of pristine PP- and nTi-PP nanocomposite melt-electrospun fibers was found average as 700 ± 0.3 and 800 ± 0.4 nm, respectively. Before functionalization with nTi, the surface of fabrics was activated by a technique using glutaraldehyde (GA) and polyethyleneimine to improve decomposition activity. Scanning electron microscopy (SEM) results revealed that titanium nanoparticles were deposited uniformly on the nanofibers. X-ray photon spectroscopy (XPS) results confirmed the presence of titanium nanoparticles and generation of amine groups after modification. Photocatalytic performance of nTi-loaded pristine and nanocomposite melt-electrospun filters was investigated by using methyl orange (MO) as a model compound. The decolorization experiments were carried out by varying initial dye concentration (10, 20, 40 mg/L), pH (2, 5, and 9), and loaded TiO_2 amount (1 and 2 %). According to photocatalytic decolarization test results, nTi-loaded GA-treated pristine or nTi-PP nanocomposite fabric filter has better properties compared to GA-untreated group from point of photocatalytic efficiency, especially over 90 % decolorization efficiency at GA-treated pristine and nTi-PP composite PP fabrics. The complete decolarization of MO was observed at pH value of 5, photocatalyst concentration of 20 mg/L, and 1 % nTi-loading after 3 h. The results show that surface activated PP nonwovens, which is introduced Ti nanoparticles into and onto the structure, a good photocatalytic activity.

Keywords Titanium oxide nanoparticles · Polypropylene · Photodegradation · Methyl orange · Polyethyleneimine · Glutaraldehyde

Z. Karahaliloglu
Nanotechnology and Nanomedicine Division, Hacettepe University, Beytepe, 06800 Ankara, Turkey

C. Hacker · G. Seide · T. Gries
Institut fuer Textiltechnik der RWTH Aachen University (ITA), 52074 Aachen, Germany

M. Demirbilek
Advanced Technologies Research and Application Center, Hacettepe University, Beytepe, 06800 Ankara, Turkey

E. B. Denkbas (✉)
Biochemistry Division, Department of Chemistry, Hacettepe University, Beytepe, 06800 Ankara, Turkey
e-mail: denkbas@hacettepe.edu.tr

Introduction

Textile industry is one of the fastest growing industries, but this important industry has come with a lot of

problem such as water, air and solid waste pollutions. Most important problem for textile industry is discharging into the water of the used dyestuff during textile processing. The generated dye wastes become a threat in terms of human health. Additionally, these dyes can threat the ecosytem because of generated byproducts (aromatische amine) (Aksu and Çağatay 2006) or the light needed of aquatic organisms for photosynthesis are inhibited due to dyestuff through the water surface. Among mentioned dyes, especially reactive azo dyes are highly hazardous substances, which are widely used in textile industry (Park and Choi 2003; Nillson et al. 1993). Therefore, the decolorization of the dyeing wastewater is a most important problem, especially with azo dyes.

Recently, the removal of dyes from wastewater has been realized by chemical and physical methods such as chemical coagulation, flocculation, precipitation, and ozonation (Chanathaworn et al. 2012; Ong et al. 2011). Among them, ozonation is very costly and causes concreted sludge in water systems. Therefore, alternative methods are needed for the wastewater treatment. Titanium-mediated photocatalysis is a growing research interest for few years because of their best photocatalyst performance (Blake 1995; Al-Qaradawi and Salman 2002). In the process, electrons and holes in the valance and conduction band are excited by visible light. They migrate to the surface of TiO_2 particles and serve as redox sources that leading to the formation of highly reactive species such as superoxide radical anions, hydrogen peroxide, and hydroxyl radicals. The reactive species can oxidize the organic compounds like dyes in the aqueous solution to CO_2 and H_2O (Wu et al. 1998). Titanium-based photodegradation of dyeing wastewater provides not only effective degradation process but also degradation of dye without undesirable byproducts. Moreover, this photocatalytic property includes materials indicate bactericidal effect (Grassian 2005).

PP fibers have been widely used in the fields of textiles, automobiles, protective coating, battery separator, and filtration because of their attractive properties such as hydrophobicity, good mechanical strength, chemical resistance, and low-cost production (Karger-Kocsis 1999; Noumowe 2005; Kim et al. 2009; Lee and Obendorf 2007). The electrospinning process of PP from solution has limited success because of insoluble of PP in common solvents at room temperature (Lee et al. 2009). However, PP has no reactive functional groups, and its disadvantage limits the use in different numerous applications (Hung et al. 2008). In contrast to solution electrospinning, melt-electrospinning technique does not need a solvent. This situation comes with a lot of privileges such as the minimization of production cost, environmental pollution, and cellular toxicity depends on the use of organic solvent (Dalton et al. 2006, 2008). Therefore, melt-electrospinning is a best way for thin fiber production through electrospinning from PP.

Surface functionalization of the nanostructured materials is of great interest. For the modifications of polymeric fibers, nanoparticles such as TiO_2, MgO, and Al_2O_3 have been recently incorporated into or onto the nanofibers. During electrospinning process, the obtained nanocomposite membrane due to the nanoparticles mixed with polymer solution shows not good performance because of embedding of the nanoparticle into nanofibers. As another possibility, the electrospinning of polymers and the surface modification of their nanoparticle, which is called as electrospraying, were performed simultaneously. But this method has a disadvantage that the stability of nanoparticle-based nanofibers through electrospraying may be poor (Balamurugan et al. 2011). From this reasons, the existence of functional group on the nanofiber surface becomes necessary in order to decorate of surface with nanoparticels (Yanga et al. 2012; Garcia and Galindo 1990).

In this study, nTi/PP nanocomposite and pristine PP fabrics were prepared by melt-electrospinning. Melt-electrospinning parameters were optimized. $-NH_2$ groups were created on melt-electrospun pristine or nTi-PP composite fabric by treatment with glutaraldehyde and PEI to assess of the filtration efficiency and improve the bonding capacity of titanium nanoparticles onto the surface. The resulting fiber fabrics were characterized, and the thermal and morphological properties of theirs were presented. The effects of titanium nanoparticle localization and amine modification on the dye degradation were investigated. The applicability of the chemical-activated composite and pristine fibers for a novel treatment of dyeing wastewater was evaluated.

Experimental

Materials

Titanium (IV) oxide nanoparticles (Alfa Aesar-45603) consist of 99.7 % of the anatase crystal form were supplied by Sigma-Aldrich for the modification of melt-electrospun filters. The dimension of titanium (IV) oxide nanoparticles is ca. 15 nm. Polypropylene (i-PP) granules were obtained from Borealis (Gent, Belgium). Methyl orange (MO) was used as model compounds for the assessment photocatalytic decolorization of pristine PP and nTi-PP nanocomposite fabrics. UV lamp with a wavelength of 312 nm and of 8 W power was used as a light source in this study.

Preparation of nTi-PP nanocomposite

Initially, titanium nanoparticles and sodium stearate (SS) which increase the electrical conductivity of the polymer and melt and facilitate the electrospinning process were added into PP granules in the ratio of 1:95:4 (wt%) (TiO_2:PP:SS) and were mixed to disperse particles in a rotator for 3 h. The obtained mix was dried at 120 °C for 24 h to remove the adsorbed water.

A twin-screw extruder was used for preparation of nTi-PP composite. The process temperature was set as 190 °C, and the speed of the screw was 80 rpm/min. From the prepared nTi-PP nanocomposite melts, i.e., from the extruded melts, strips which have 50-mm average width and 0.5-mm thickness were prepared by injection molding machine in order to minimize the generation of air bubble during melt-electrospinning process. Cross-sectional images of the prepared PP strips were obtained using scanning electron microscopy (SEM, Quanta 200 FEG).

Preparation of pristine PP and nTi-PP nanocomposite melt-electrospun fabrics

A melt-electrospinning setup, which includes a high voltage supply (Eltex 50 kV static charging system), syringe pump (Harvard Apparatus 11 Plus), two heating system for the polymer melt reservoir, and nozzle and collector were used in this study (Hacker et al. 2014). PP and nTi-PP composite strips were loaded into the glass syringe surrounded by a circular heating tube made of stainless steel and were heated until completely molten approximately for 30 min. The molten polymer was exposed to second heating zone (heating plate around metallic nozzle) when the polymer was pushed toward collector (diameter 7 cm, made of aluminum). Both heating zone temperatures are adjustable up to 400 °C. The best processing conditions (applied voltage, collecting distance, and flow rate) for the both materials (pristine PP and nTi-PP nanocomposite fabrics) in terms of electrospun ability were examined.

SEM (JEOL JSM700F) was used for observing the morphology of pristine PP and nTi-PP composite melt-electrospun fabrics. The average fiber diameter was determined by measuring diameters of fibers at 500 points from approximately eight images taken per area using image-processing software (ImageJ, NIST).

Surface modification and characterization

The surface of pristine and nTi-PP nanocomposite fabrics was modified as chemically according to Garcia's method (Garcia and Galindo 1990). Firstly, melt-electrospun PP fabrics were cut into disk shape of 1-cm diameter. The samples having a surface area of 0.785 cm^2 were immersed in 10 mL of a 5 % (v/v) solution of glutaraldehyde in water for 2 h at 70 °C on a heating magnetic stirrer. Thereafter, the samples were thoroughly washed twice with deionized water. The samples were immersed in 3 mL of a 5 % (w/v) PEI solution in water at 40 °C for 2 h with agitating and washed again with deionize water. PP fabrics were characterized by attenuated total internal reflectance infrared spectroscopy (ATR-FTIR) whether the surface was activated with glutaraldehyde and polyethylenimine.

After chemical surface modification, PP fabrics were immersed in water containing 1 and 2 % (w/v) titanium dioxide nanoparticle suspension, and the samples were sonicated at 40 °C for 2 h and kept for 1 h under agitation (Jaworek et al. 2009), and the fabrics were washed for a few times to remove unbound titania. The surface morphology of the nTi-loaded PP fabrics was observed using SEM. In order to examine the existence of titanium nanoparticles in or on the PP nonwoven fabrics and amine groups after modification, X-ray photoelectron spectroscopy (XPS, Thermo Scientific K-Alpha, USA) was used.

Thermal properties of nTi-loaded or unloaded nanocomposite and pristine PP fabric were

investigated using Differential Scanning Calorimetry (DSC, Mettler Toledo DSC-1). The samples were heated between 25 and 250 at 10 °C/min under nitrogen atmosphere. The melting temperature (T_m) and the crystallization degree (X_c) of fabrics were obtained. The degree of crystallization was calculated according to Eq. (1), where $\Delta H_0 = 209$ J/g is the melting heat of 100 % crystalline PP (Dastjerdi et al. 2010).

$$X_c = H_m/\Delta H_0. \quad (1)$$

Decolorization analysis

In the photocatalysis studies, methyl orange dye was used as model compound. The time-dependent change by the dye concentration was determined using Nanodrop 1000 Spectrometer (Thermo Scientific). Calibration curve of the dye solution (linear, $R^2 = 0.998$) was obtained from the dye solutions at various concentrations. Methyl orange dye in water showed two peaks, which is stronger peak at 461 nm and another one at 273 nm, and all data were obtained at 461 nm.

Decolorization experiments of the prepared dye solution were carried out using a light source that has 4×8W UV lamps with a wavelength of 312 nm. The test arrangement was installed by placing the glass beakers on the 4 UV lamps-covered glass plate. In all conditions, irradiation tests were performed in the glass beaker containing 3 mL of the different concentration methyl orange solution. During photodegradation study, 20 µl of sample solution was taken from the glass beaker for every 30 min and the absorbance of the solution was read using Nanodrop. For the evaluation of each parameter (the concentration of dye and nTi, pH), the plot of C/C_0 (where C and C_0 describes the concentration of dye solution at time t and initially) was observed. Decolorization efficiency of PP fabric at irradiation time was calculated by Eq. (2)

$$\text{Decolorization efficiency } (\%) = (C_0 - C/C_0) \times 100. \quad (2)$$

Results and discussions

Characterization of PP fabrics

Uniform pristine PP fabrics were prepared successfully by using additive (4 wt%), i.e., sodium stearate. The process parameters were determined as 25 kV, a working distance of 5 cm, a feed rate of 0.1 mL/h, and a temperature of thermocouple and hot coil of 210–305 °C. The surface morphology of the pristine PP fabrics is shown in Fig. 1a. The average diameter of pristine PP melt-electrospun fabrics was measured approximately 700 ± 0.3 nm (Fig. 1b).

Figure 2a represents the morphology of titanium nanoparticles. These nanoparticles having a diameter 15 nm are in clusters as observed in high magnification SEM image. But, as shown in Fig. 2c, the

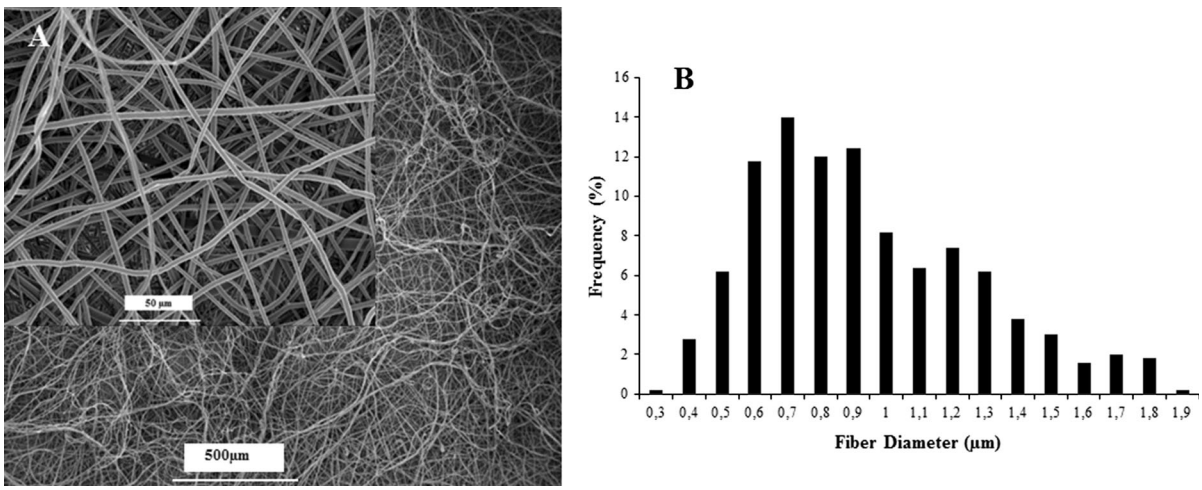

Fig. 1 (**A**) SEM image of pristine melt-electrospun PP fabric. The *inset* shows higher magnification image of the surface, (**B**) Diameter distribution of the prepared pristine melt-electrospun PP fabric. Pristine melt-electrospun PP fabric with a diameter 700 ± 0.3 nm was obtained. *Scale bars* are 50 and 500 µm

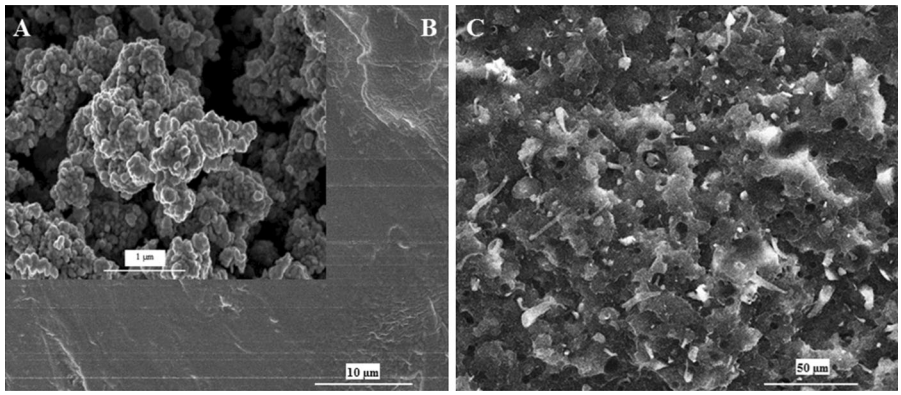

Fig. 2 SEM image of the commercial titanium nanoparticles (**A**), cross-sectional images of the prepared pristine PP strips (**B**), and nTi-PP nanocomposite strip after compounding (**C**). *Scale bars* are 1, 10 and 50 μm

presence of nTi on the surface of the composite strip is relatively apparent compared to cross-sectional image of pristine PP strip (Fig. 2b) and although there are several aggregation points for the nanoparticles, the nanoparticles distribute generally uniformly in PP powder.

Similarly to pristine PP, nTi-PP composite fabrics were prepared by melt-electrospinning after mixing sodium stereate, Ti nanoparticles, and polypropylene granule (4:1:95 wt%). The average diameter of nTi-PP nanocomposite fabrics which were fabricated by thermocouple/hot coil temperature of 260/300, flow rate of 0.07 mL/h, distance of 5 cm and 30 kV, as shown in Fig. 3a, was 800 ± 0.4 nm. The electrospin process of nTi-PP composite was carried out successfully with desired morphological characteristics in spite of defects in the form bead in some of the fiber (Fig. 3).

After preparation of PP fabrics, the surface was activated by a technique using glutaraldehyde and polyethyleneimine for increasing of titanium nanoparticle binding efficiency. ATR-FTIR spectra of pristine PP fabric, as shown in Fig. 4, are in accord with the unique absorption peaks of –CH, –CH2, $–CH_3$ at 2,925 cm^{-1} and $–CH_2$, $–CH_3$ at 1,458 cm^{-1}, 1,377 cm^{-1} in the literature (Huang et al. 2011). After polyethylenimine modification, obtained peaks of 3,200 and 1,620–1,660 cm^{-1} can attribute to NH_2 group and Schiff base group (C=N group) (Garcia and Galindo 1990). For the amine modification, two different concentrations, which are 5 and 20 %, were examined, but the fiber structure of PP fabrics becomes deformed when glutaraldehyde solution of 20 % was used. Therefore, at glutaraldehyde concentration of 5 %, the successfully surface modifications were carried out as it is also seen from ATR-FTIR spectra.

Figure 5 presents SEM images of the PP fibers with loaded titanium nanoparticles (1 %) after and before glutaraldehyde modifications. Clearly, PP fabrics without GA-treatment exhibit lower deposited particles compared to treated group (Fig. 5a). After modification, at 1 wt% loading of the nanoparticles, the surface of pristine PP fabric and nTi-PP nanocomposite is densely covered by finely dispersed nTi, as revealed in Fig. 5b, c. Therefore, GA-treatment is a feasible and efficient method to Ti-deposition.

The DSC results of the fabrics are given in Table 1. As can be seen in results, melt temperature of PP fabrics was reduced slightly with melt-electrospinning process. The degree of crystality of the modified pure and composite PP fabric (1 % nTi-loaded group) was decreased with increase of titanium oxide nanoparticle concentration. The reduction in crystallinity of fabrics including TiO_2 nanoparticles can be associated to the physical hydrance effect of titanium oxide nanoparticle on the motion of the polymer chains (Dastjerdi et al. 2008; Chiu et al. 2011). But 2 % nTi-loaded nanocomposite fabric shows higher crystallinity degree (31 %) and melting temperature compared to 2 % nTi-loaded pristine PP fabric that this situation can be attributed to not allowing the more loading of titanium dioxide nanoparticle after GA modification at composite group depends on change of surface charge properties. On the other hand,

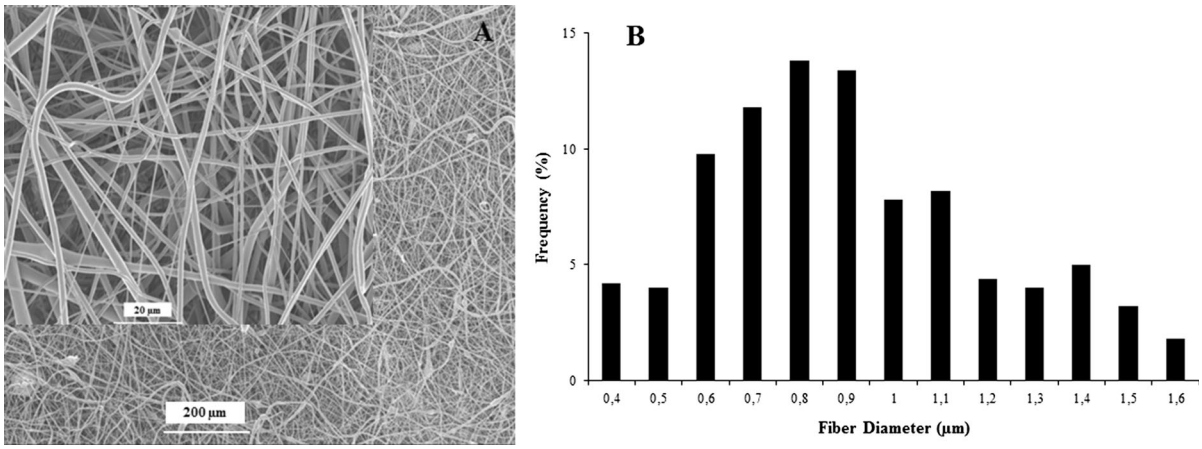

Fig. 3 (**A**) SEM image of the melt-electrospun nTi-PP nanocomposite fabric. The *inset* shows higher magnification image of the surface, (**B**) Diameter distribution of the prepared melt-electrospun nTi-PP nanocomposite fabric. nTi-PP composite fabric with a diameter 800 ± 0.4 nm was obtained. *Scale bars* are 20 and 200 µm

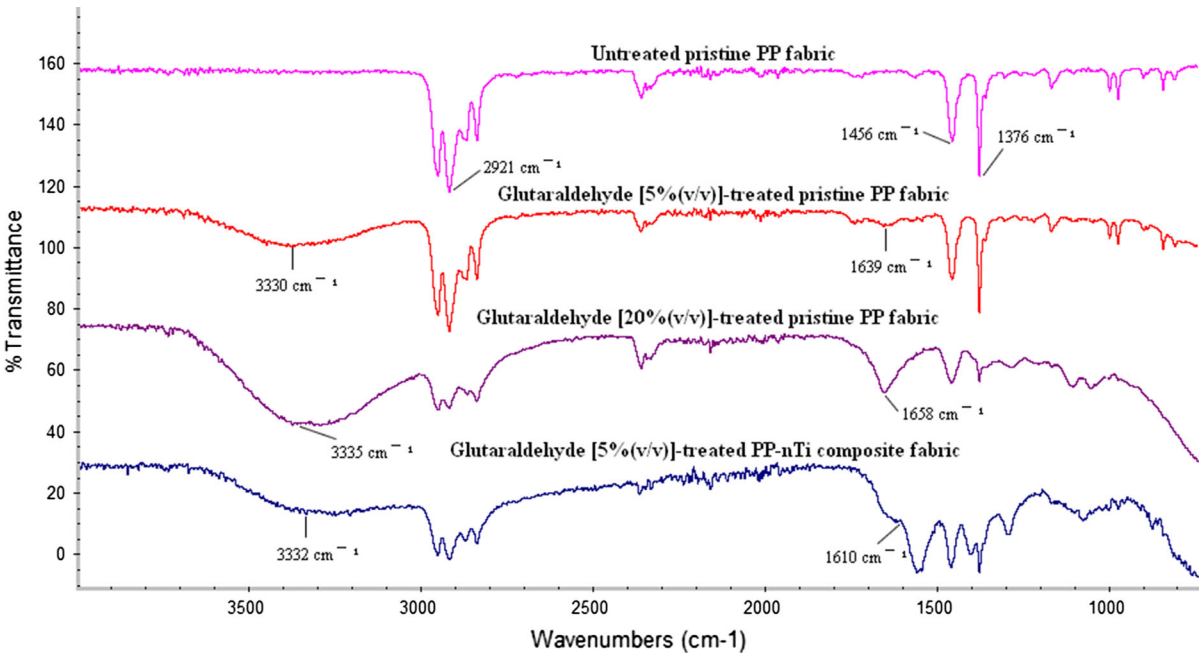

Fig. 4 ATR-FTIR spectra of pristine PP, GA-treated pristine PP, and nTi-PP nanocomposite fabrics. Carbonyl-terminated nonwoven PP fabric was obtained by glutaraldehyde treatment, and then these groups were reacted with PEI

crystallization degree of 1 % nTi-loaded GA-treated PP and composite fabric is lower than 2 % nTi-deposited group. The increase in crystallinity at loaded PP fabric with high nTi-concentration (2 %) revealed that the amount of attached nanoparticles to the surface was reduced with increase titanium nanoparticles concentration. DSC results of the pristine and composite PP fabrics are in good agreement with nTi-concentration-dependent photodegradation efficiency.

Figure 6 shows the XPS results of GA-treated or non-treated pristine and composite PP fabrics. As seen in XPS spectra for Ti 2p of nTi-loaded GA-treated pristine and nTi-PP composite fabrics, the signals at

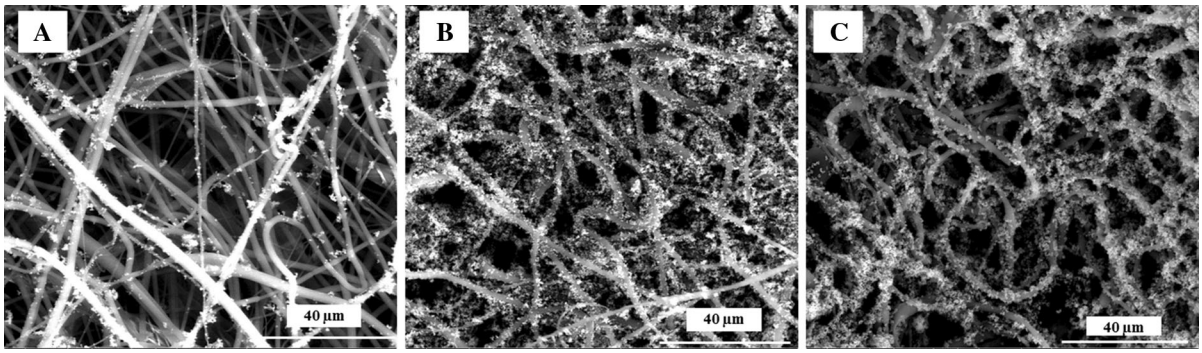

Fig. 5 SEM images of nTi-loaded pristine PP fabrics without surface modification (**A**), nTi-loaded pristine PP fabric (**B**), and nTi-PP nanocomposite fabric after surface modification (**C**). The surface of GA-treated fabrics shows more deposited titanium nanoparticles compared to untreated group. *Scale bars* are 40 µm

Table 1 Thermal properties of the samples. The crystallinity of PP fabrics including TiO_2 nanoparticles reduced

Material	T_m (°C)	ΔH_m (*J/g*)	X_c (%)
PP granule	164.23	87.44	41.83
Pristine PP fabric	159.36	85.57	40.94
nTi-PP composite fabric	159.20	62.16	29.74
1 % nTi-loaded GA-treated pristine PP fabric	158.87	31.85	15.23
2 % nTi-loaded GA-treated pristine PP fabric	159.63	53.67	25.67
1 % nTi-loaded GA-treated PP-nTi composite fabric	159.57	38.97	18.64
2 % nTi-loaded GA-treated PP-nTi composite fabric	160.06	66.79	31.95

463.78 and 457.68 eV are corresponding to Ti $2p_{1/2}$ and Ti $2p_{3/2}$ orbitals, respectively (Sheikh et al. 2010; Drew et al. 2003). Table 2 shows atomic percentage of carbon, oxygen, nitrogen, and titanium on the surface of PP fabrics. The presence of N1s peak at 398.4 eV in the surface scan of XPS spectra of GA-treated pristine or composite PP fabric and the N atomic ratio in Table 2 demonstrated that the modification process was successful (Zhu et al. 2002). In addition to this, more nTi-binding efficiency is obtained at GA-treated group compared to GA-untreated group. Moreover, N1s peak intensity of nTi-loaded GA-treated composite PP fabric from scans is higher than nTi-loaded pristine PP fabric. This can be associated with more titanium particles binding to nTi-PP pristine fabric with GA modified compared to composite PP fabric with GA modified and the existence of amine-OH groups on the GA–treated composite group. These results are confirmed with DSC and photocatalytic results.

The time-dependent decolorization efficiency of the MO solution under three different concentrations (10, 20, 40 mg/L) was investigated. Figures 7, 8, and 9 show the change of the methyl orange dye concentration in solution by photo-decolorization with irradiation time. As can be seen in Fig. 7, the color of the methyl orange solution becomes colorless after 150 min at the GA-treated composite, and pristine PP fabrics become colorless after 330 min at nTi-loaded untreated pristine PP fabric at 10 mg/L. nTi-loaded GA-untreated nTi-PP composite fabric can decompose dye solution approximately 210 min later than GA-untreated pristine PP fabric.

As shown in Figs. 8 and 9, at dye concentration of 20 mg/L, for nTi-loaded treated pristine and composite PP fabric, total decomposition of the dye occurs after 180 min. But untreated groups can be carried out the decolorization of the dye after about 240 min from the treated group. Between treated pristine and composite PP fabric, the significant difference in terms of decomposition rate is not shown, although modified pristine PP fabric indicates faster decolorization tendency compared to composite PP fabric. Among untreated groups, untreated PP pristine fabric exhibits higher photocatalytic decolorization performance under dye concentration of 20 mg/L as well as at dye concentration of 10 mg/mL. Treated nTi-PP composite and pristine PP fabric at 10 mg/L of dye concentration become colorless earlier 30 min than

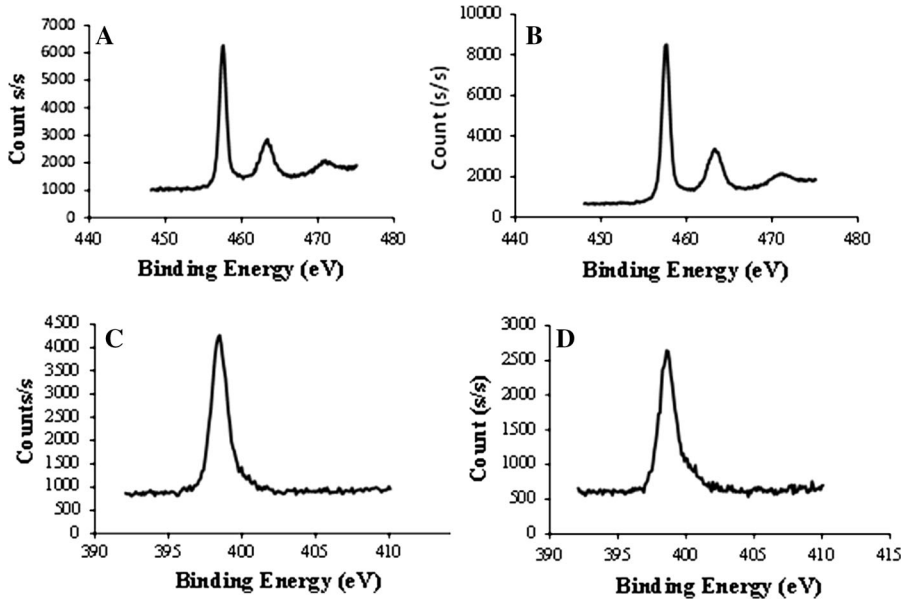

Fig. 6 XPS spectra of Ti2p (**A**, **B**) and N1s (**C**, **D**), by GA-treated pristine PP (**B**, **D**) and composite (**A**, **C**) which loaded with TiO_2

Table 2 Atomic ratio of carbon, nitrogen, oxygen, and titanium on the surface of PP fabric determined by X-ray photoelectron spectroscopy. nTi-binding efficiency at GA-treated groups increased compared to GA-untreated groups

Atomic percent	C	O	Ti	N
Pristine PP fabric	95.93	4.07	–	–
nTi-PP composite fabric	97.01	2.99	1.28	–
1 % nTi-loaded GA-treated nTi-PP composite fabric	63.38	15.78	6.43	14.4
2 % nTi-loaded GA-treated pristine PP fabric	46.28	26.76	12.13	10.66
1 % nTi-loaded GA-untreated nTi-PP composite fabric	82.51	11.45	3.98	–
2 % nTi-loaded GA-untreated pristine PP fabric	77.26	14.14	5.92	–

20 mg/L when dye concentration of 10 mg and 20 mg/L was compared in terms of decomposition activity. Untreated PP fabric in dye solution of 10 mg/L exhibits higher efficiency than that of 20 mg/L. Photocatalytic removal efficiency of fabrics decreases with the increased initial concentration of dyes, which depends on increase of the dye amount adsorbed on the catalyst surface of fabrics followed inhibition of the light penetration by dye molecules (Nam et al. 2002; Carter et al. 2000; Malato et al. 1998). The obtained results are good agreement with this information.

Results presented in Fig. 10 show that at dye concentration of 40 mg/L, the decolorization rate of each experiments group was reduced, and nTi-loaded GA-treated pristine and composite PP fabric can decompose the dyes after 9 h of UV-illumination when untreated group indicates lower performance in terms of decolorization of the solution (approximately 18 h). nTi-loaded GA-treated group shows two times higher performance compared to untreated samples.

Dye concentration of 20 mg/L shows the strongest decolorization among different dye concentrations as photocatalysts; it is more favorable from the point of degradation efficiency. Therefore, the adsorption of dye onto PP fabrics was carried out at different pH values at concentration of 20 mg/L. The photocatalytic performances of fabrics were observed at pH values of 2, 5, and 9.

pH plays important role on titanium-mediated photocatalysis. Reports show that photocatalytic activity increases with decrease of pH value , i.e., titanium-mediated photocatalysis rate is higher in acidic media (Saggioro et al. 2011; Barka et al. 2008; Guettai and Amar 2005). This situation can be attributed to the surface charge of TiO_2. The surface charge of TiO_2 is positively charged at lower pH values (Evgenidou et al. 2005; Wei et al. 2009). Photodegradation efficiency is depending on anionic or cationic form of the used dye. Methyl orange is an anionic dye; thereby decolorization rate was expected

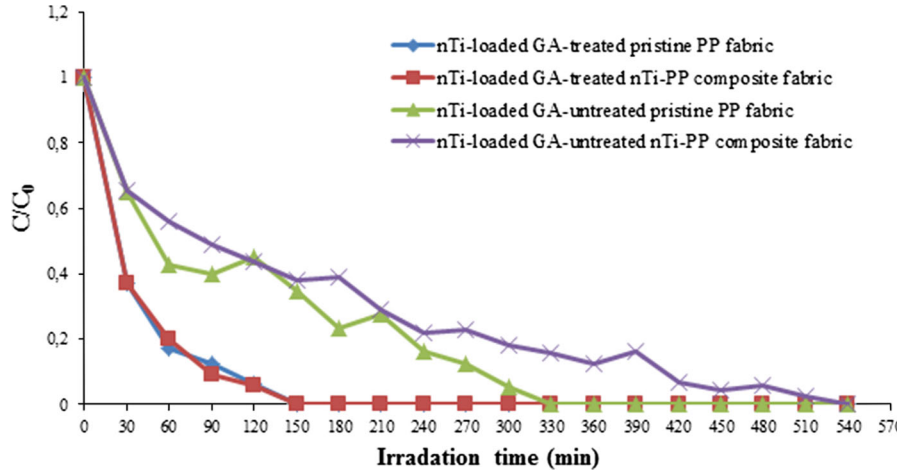

Fig. 7 Decolorization results of MO dye solution at 10 mg dye/L, pH 5, and 1 wt% TiO_2. The color of the methyl orange solution became colorless after 150 min at the GA-treated fabrics

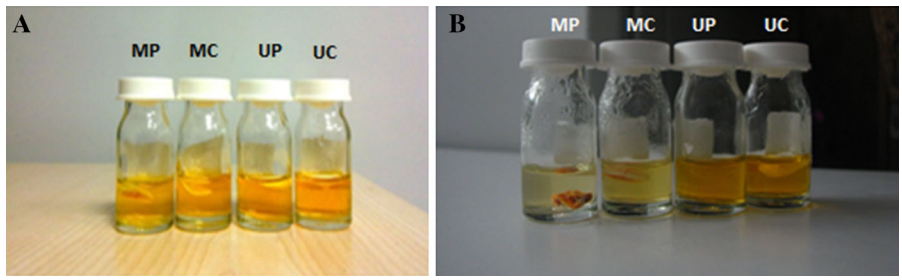

Fig. 8 The change at the dye concentration, (**A**) initially, (**B**) after 60 min at 20 mg/L of dye concentration, pH 5, and 1 wt% TiO_2. (*MP:* nTi-loaded modified pristine PP fabric; *MC:* nTi-loaded modified composite PP fabric; *UP:* nTi-loaded unmodified pristine PP fabric; *UC:* nTi-loaded unmodified composite PP fabric)

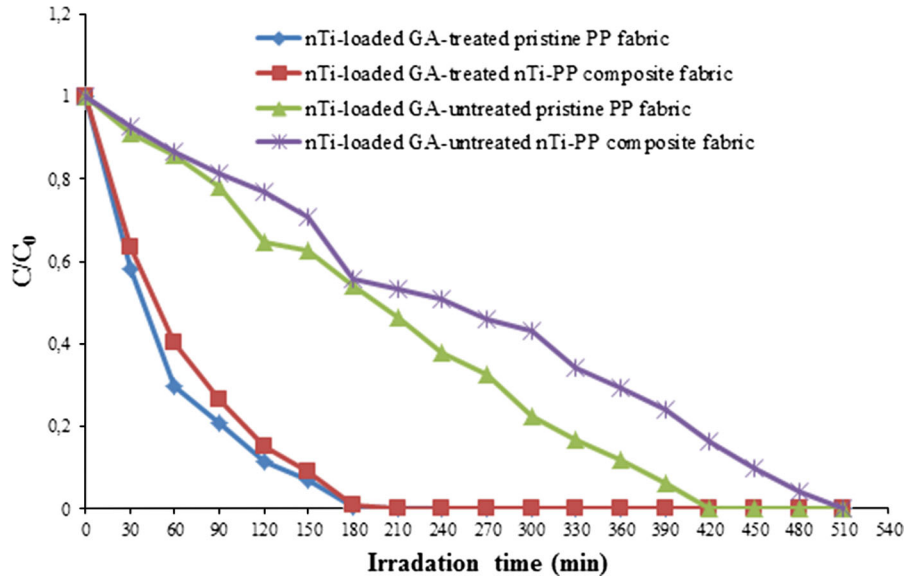

Fig. 9 Decolorization results of MO dye solution at 20 mg dye/L, pH 5, and 1 wt% TiO_2. The untreated group carried out the decolorization of dye after about 240 min from the treated group

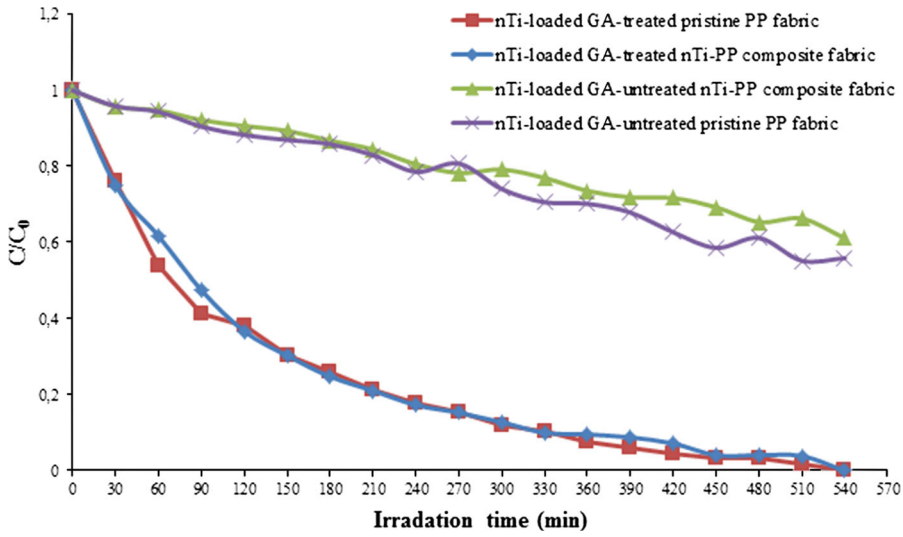

Fig. 10 Decolorization results of MO dye solution at 40 mg dye/L, pH 5, and 1 wt% TiO_2. nTi-loaded GA-treated group shows two times higher performance compared to untreated samples in terms of decolorization of the solution

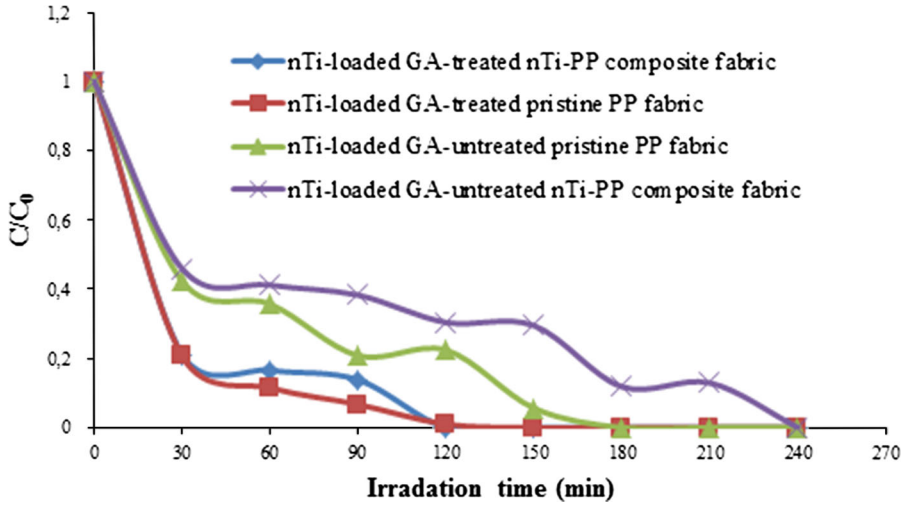

Fig. 11 Decolorization results of MO dye solution at 20 mg dye/L, pH 2, and 1 wt% TiO_2. GA-treated pristine and composite at pH value of 2 show higher decolorization efficiency compared to pH 5

to be higher at the lower pH value because of electrostatic interaction between titanium nanoparticle and dye. Figures 11 and 12 show the removal efficiency of dye solution at pH value of 2 and 9. As can be seen in Fig. 11, nTi-loaded GA-treated composite and pristine PP fabric are not significantly different in terms of cleaning of the dye solution. GA-treated composite or pristine PP fabrics at pH value of 2 indicate high decolorization efficiency compared to pH 5 which is earlier 1 h. Similarly, untreated group, specially composite fabric at pH 2, can decolorize the solution earlier 4, 5 h compared with pH 5. The decrease at pH value affects the untreated group more than treated group, and the dye can be degraded strongly fast by composite PP fabric.

The decomposition results at pH value of 9 are presented in Fig. 12. In all samples, decrease of decomposition rate depends on negatively charge of the surface of titanium dioxide at high pH value. After approximately 9 h of UV–Vis illumination, completely decolorization effect was observed at the GA-treated composite PP fabric. nTi-loaded treated composite or pristine group can decompose the dye 5 h earlier than nTi-loaded GA-untreated composite PP fabric.

To shown the change by decolorization time with increase of titanium nanoparticles, concentration was examined by nTi-loading of 2 wt% of PP fabrics. According to previous studies, photocatalytic activity increases with increase of the number of titanium

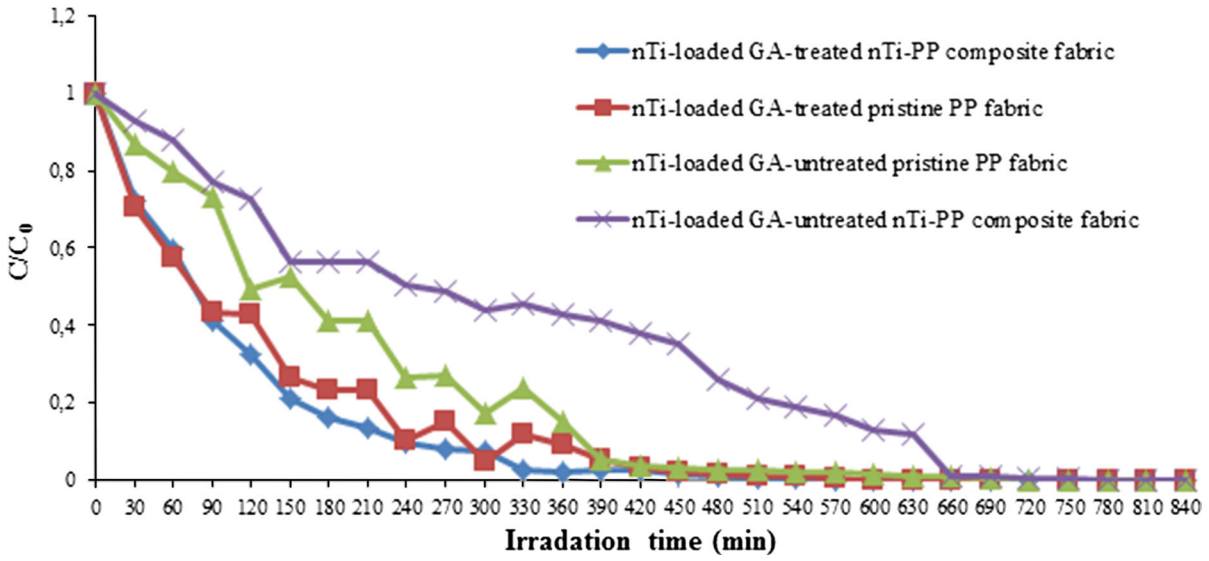

Fig. 12 Decolorization results of MO dye solution at 20 mg dye/L, pH 9 and 1 wt% TiO_2. GA-treated PP fabric decomposes the dye after approximately 9 h

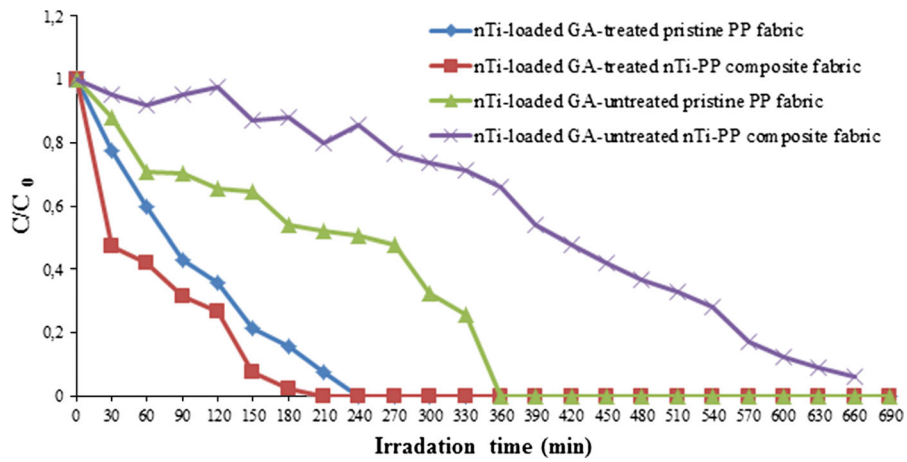

Fig. 13 Decolorization results of MO dye solution at 20 mg dye/L, pH 5, and 2 wt% TiO_2. 2 wt% nTi-loaded GA-treated pristine fabric decomposes the dye after 1 h from 1 % loading

nanoparticles, which depends on increase the number of absorbed photons. As can be seen in Fig. 13, decolorization time is decreased by the excessive amount of nTi. The complete degradation of MO was observed 1 h earlier at nTi-loading of 2 wt% compared to 1 wt% nTi-loaded GA-untreated pristine PP fabric. But, when the presence of photocatalyst is too much, light penetration becomes difficult and decreases the photocatalytic activity (Zhu et al. 2012; Nishio et al. 2006). nTi-loading of 2 wt% GA-treated pristine fabric decomposes the dye after 1 h from nTi-loading of 1% (wt) because of the presence of excess titanium nanoparticles.

Figure 14 summarizes the percentage of decolorization efficiency of PP fabrics under the different dye and titanium nanoparticle concentrations and pH in terms of decolorization efficiency. After 2 h of exposure, the decolorization percentage of dye solution (10 mg/L) was reached above 90 % by the GA-treated pristine PP fabric. The efficiency percentage decreases with increase of concentration of the dye that GA-treated group has the lower activity when compared with another dye concentration. On the basis of obtained results of decolorization efficiency at different pH values, the use of treated pristine PP fabric yielded a 100 % reduction at pH

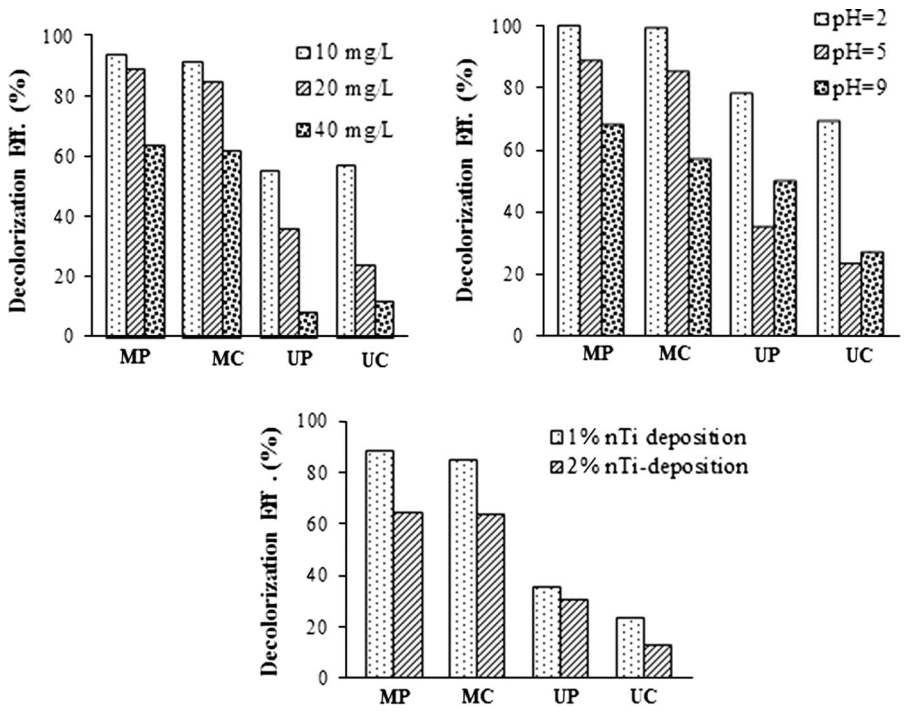

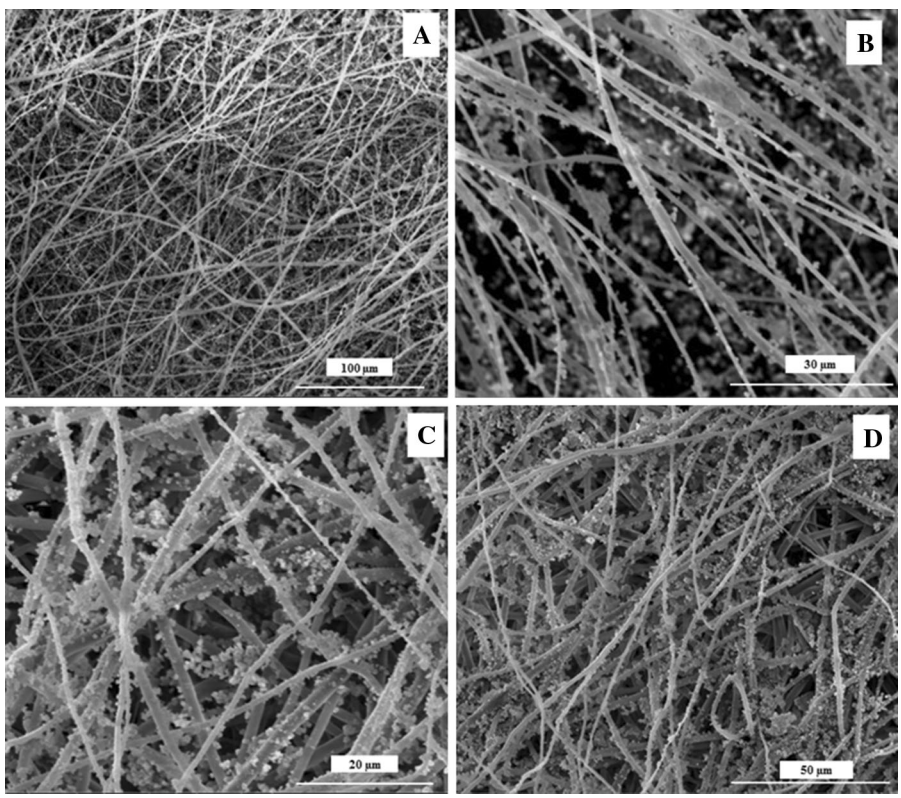

Fig. 14 Decolorization efficiency of MO by modified or unmodified PP fabric after 120 min. nTi-loaded GA-treated pristine or composite PP fabrics show the highest removal efficiency

Fig. 15 SEM images at dye concentration of 20 mg/L, pH value of 5 and 1 % nTi-loading after 540 min (**A**) MP, (**B**) MC, (**C**) UP, (**D**) UC. nTi maintains the existence on the surface after 540 min of decolorization

value of 2 after 2 h. It is interesting to note that degradation efficiency of untreated group is increased at low and high pH values. The photodegradation efficiency of untreated composite PP fabric is increased from 23 to 69 % when pH value is decreased from 5 to 2. But nTi-loaded GA-treated pristine or composite PP fabrics show the highest removal efficiency in all pH and concentration values.

At Fig. 15, SEM images of all samples at dye concentration of 20 mg/L after 540 min are given. nTi maintains the existence on the surface without any loss during decolorization experiments. From this result, it seems that prepared PP fabrics can be reused.

Conclusions

In this paper, for the decoration of PP fabrics with titanium nanoparticle, two methods were used which are the incorporation titanium oxide nanoparticles into PP fabrics during melt-electrospinning or binding on the surface of titanium oxide nanoparticle. But this binding was very poor because of the lack of the functional group. Therefore, the surface was modified by glutaraldehyde and polyethylenimine. Results of the SEM and XPS analysis indicated that titanium nanoparticles were successfully deposited on melt-electrospun PP fabric due to the chemical activation of surface. According to the decolorization results, the methyl orange decolorization rate among the samples was occurred in the following order MP > MC > UP > UC at pH value of 5, nTi and dye concentration of 1 % and 20 mg/L that this value was determined as optimum dosage in terms of decomposition performance. nTi-loaded GA-treated PP pristine fabric achieved decolorization over 90 % at pH value of 5, photocatalyst concentration of 20 mg/L, and 1 % nTi-loading after 3 h. Based on sample size and low surface area, the obtained photocatalytic activity results for nTi-loaded GA-treated groups are useful and helpful in designing an effective filter production for dye wastewater treatment. This study clearly shows nTi-loaded GA-treated composite or pristine PP fabric can be used as photocatalytic filter to decolorization of wastewater and purify environment because of better photocatalytic activity properties.

Acknowledgments The authors are grateful to Tayfun Vural from Hacettepe University for the considerable assistance regarding the analytical methods.

References

Aksu Z, Çağatay SS (2006) Investigation of biosorption of Gemazol Turquise Blue-G reactive dye by dried *Rhizopus arrhizus* in batch and continuous systems. Sep Purıf Technol 48:24–35. doi:10.1016/j.seppur.2005.07.017

Al-Qaradawi S, Salman RS (2002) Photocatalytic degradation of methyl orange as a model compound. J Photochem Photobiol A 148:161–168. doi:10.1016/S1010-6030(02)00086-2

Balamurugan R, Sundarrajan S, Ramakrishna R (2011) Recent trends in nanofibrous membranes and their suitability for air and water filtrations. Membranes 1:232–248. doi:10.3390/membranes1030232

Barka N, Assabbane A, Nounah A, Dussaud J, Ichou YA (2008) Photocatalytic degradation of methyl orange with immobilized TiO_2 Nanoparticles: effect of pH and some inorganic anions. Phys Chem News 41:85–88

Blake DN (1995) Bibliography of work on the heterogeneous photocatalytic removal of hazardous compounds from water and air, document NREL/TP-473-20300. National Renewable Energy Laboratory/DOE, Golden Co, Golden

Carter SR, Stefan MI, Bolton JR, Safarzadeh-Amiri A (2000) UV/H_2O_2 treatment of methyl tertbutyl ether in contaminated waters. Environ Sci Technol 34:659–662. doi:10.1021/es9905750

Chanathaworn J, Bunyakan C, Wiyaratn W, Chungsiriporn J, Songklanakarin J (2012) Photocatalytic decolorization of basic dye by TiO_2 nanoparticle in photoreactor. Sci Technol 34:203–210

Chiu CW, Lin CA, Hong PD (2011) Melt-spinning and thermal stability behaviour of TiO_2 nanoparticle/polypropylene nanocomposite fibers. J Polym Res 18:367–372. doi:10.1007/s10965-010-9426-0

Dalton PD, Klinkhammer K, Salber J, Klee D, Moeller M (2006) Direct in vitro electrospinning with polymer melts. Biomacromolecules 7:686–690. doi:10.1021/bm050777q

Dalton PD, Joergensen NT, Groll J, Moeller M (2008) Patterned melt electrospun substrates for tissue engineering. Biomed Mater 3:034109. doi:10.1088/1748-6041/3/3/034109034109

Dastjerdi R, Mojtahedi MRM, Shoshtari AM (2008) Investigating the effect of various blend ratios of prepared masterbatch containing Ag/TiO_2 nanocomposite on the properties of bioactive continuous filament yarns. Fiber Polym 9:727–734. doi:10.1007/s12221-008-0114-1

Dastjerdi R, Mojtahedi MRM, Shostar AM, Khosroshah A (2010) Investigating the production and properties of Ag/TiO_2/PP antibacterial nanocomposite filament yarns. J Text Inst 101:204–213. doi:10.1080/00405000802346388

Drew C, Liu X, Ziegler D, Wang X, Bruno FF, Whitten J, Samuelson LA, Kumar J (2003) Metal oxide-coated polymer nanofibers. Nano Lett 3:143–147. doi:10.1021/nl025850m

Evgenidou E, Fytianos K, Poulios I (2005) Photocatalytic oxidation of dimethoate in aqueous solutions. J Photochem Photobiol A 175:29–38. doi:10.1016/j.jphotochem.2005.04.021

Garcia JL, Galindo E (1990) An immobilization technique yielding high enzymatic load on nylon nets. Biotechnol Tech 4:425–428. doi:10.1007/BF00159390

Grassian VH (2005) Environmental catalysis. CRC Press, Taylor & Francis Group, Boca Raton

Guettaï N, Amar HA (2005) Photocatalytic oxidation of methyl orange in presence of titanium dioxide in aqueous suspension. Part I: parametric study. Desalination 185:427–437. doi:10.1016/j.desal.2005.04.048

Hacker C, Karahaliloğlu Z, Seide G, Denkbaş EB (2014) Functionally modified, melt electrospun thermoplastic polyurethane mats for wound-dressing applications. J Appl Polym Sci 131:1–12. doi:10.1002/APP.40132

Huang KS, Lian HS, Chen JB (2011) Study on the modification of PP nonwoven fabric. Fibres Text East Eur 19:82–87

Hung C, Chuang H, Chang F (2008) Novel reactive compatibilization strategy on immiscible polypropylene and polystyrene blend. J Appl Polym Sci 107:831–839. doi:10.1002/app.25201

Jaworek A, Krupa A, Lackowski M, Sobczyk AT, Czech T, Ramakrishna S, Sundarrajan S, Pliszka D (2009) Electrostatic method for the production of polymer nanofibers blended with metal-oxide nanoparticles. J Phys 146:1–6. doi:10.1088/1742-6596/146/1/012006

Karger-Kocsis J (1999) Polyprophylene an A–Z reference. Kluwer Academic, London

Kim J, Hinestroza JP, Jasper W, Barker RL (2009) Effect of solvent exposure on the filtration performance of electrostatically charged polypropylene filter media. Text Res J 79:343–350. doi:10.1177/0040517508090887

Lee S, Obendorf SK (2007) Barrier effectiveness and thermal comfort of protective clothing materials. J Text I 98:87–97. doi:10.1533/joti.2005.0143

Lee KH, Ohsawa O, Watanabe K, Kim IS, Givens SR, Chase B, Rabolt JF (2009) Electrospinning of syndiotactic polypropylene from a polymer solution at ambient temperatures. Macromolecules 42:5215–5218. doi:10.1021/ma9006472

Malato S, Blanco J, Ritchter C, Braun B, Maldonado MI (1998) Enhancement of the rate of solar photocatalytic mineralization of organic pollutants by inorganic oxidizing species. Appl Catal B 17:347–356. doi:10.1016/S0926-3373(98)00019-8

Nam W, Kim J, Han G (2002) Photocatalytic oxidation of methyl orange in a three-phase fluidized bed reactor. Chemosphere 47:1019–1024. doi:10.1016/S0045-6535(01)00327-7

Nillson R, Nordlinder R, Wass U, Meding B, Belin L (1993) Asthma, rhinitis, and dermatitis in workers exposed to reactive dyes. Br J Ind Med 50:65–70. doi:10.1136/oem.50.1.65

Nishio J, Tokumura M, Znad HT, Kawase Y (2006) Photocatalytic decolourization of azo-dye with zinc oxide power in an external UV light irradiation slurry photoreactor. J Hazard Mater 138:106–115. doi:10.1016/j.jhazmat.2006.05.039

Noumowe A (2005) Mechanical properties and microstructure of high strength concrete containing polypropylene fibres exposed to temperatures up to 200 °C. Cement Concr Res 35:2192–2198. doi:10.1016/j.cemconres.2005.03.007

Ong S, Keng P, Lee W, Ha S, Hung Y (2011) Dye waste treatment. Water 3:157–176. doi:10.3390/w3010157

Park H, Choi W (2003) Visible light and Fe (III)-mediated degradation of acid orange 7 in the absence of H_2O_2. J Photochem Photobiol A 159:241–247. doi:10.1016/S1010-6030(03)00141-2

Saggioro EM, Oliveira AS, Pavesi T, Maia CG, Ferreira LFV, Moreira JC (2011) Use of titanium dioxide photocatalysis on the remediation of model textile wastewaters containing azo dyes. Molecules 16:10370–10386. doi:10.3390/molecules161210370

Sheikh FA, Kanjwal MA, Kim Hern, Pandeya DR, Hong ST, Kim HY (2010) Fabrication of titanium oxide nanofibers containing silver nanoparticles. J Ceram Process Res 11:685–691

Wei L, Shifu C, Wei Z, Sujuan Z (2009) Titanium dioxide mediated photocatalytic degradation of methamidophos in aqueous phase. J Hazard Mater 164:154–160. doi:10.1016/j.jhazmat.2008.07.140

Wu T, Liu G, Zhao J, Hidaka H, Serpone N (1998) Photoassisted degradation of dye pollutants. V. Self-photosensitized oxidative transformation of rhodamine B under visible light irradiation in aqueous TiO_2 dispersions. J Phys Chem B 102:5845–5851. doi:10.1021/jp980922c

Yang WJ, Yang CS, Huang CJ, Chen KS, Lin SF (2012) Bostrycin, a novel coupling agent for protein immobilization and prevention of biomaterial-centered infection produced by Nigrospora sp. No. 407. Enzym Microb Technol 50:287–292. doi:10.1016/j.enzmictec.2012.02.002

Zhu Y, Gao C, Liu X, Shen J (2002) Surface modification of polycaprolactone membrane via aminolysis and biomacromolecule immobilization for promoting cytocompatibility of human endothelial cells. Biomacromolecules 3:1312–1319. doi:10.1021/bm020074y

Zhu H, Ru J, Fu Y, Guan Y, Yao J, Xiao L, Zeng G (2012) Effective photocatalytic decolorization of methyl orange utilizing TiO_2/ZnO/chitosan nanocomposite films under simulated solar irradiation. Desalination 286:41–48. doi:10.1016/j.desal.2011.10.036